Deleted: 12

Deleted: 05

Deleted: 2017

Pulsed helium droplet beams

Deepak Verma¹, Andrey F. Vilesov^{1,2,*}

¹Department of Chemistry, University of Southern California, Los Angeles, California 90089 USA

²Department of Physics and Astronomy, University of Southern California, Los Angeles, California 90089 USA

*Corresponding contributor. E-mail: vilesov@usc.edu

Abstract

We report a systematic study of pulsed cryogenic expansion at temperatures ranging from 20 K down to 4.5 K, which enables us to span a large range of helium droplet sizes from $\sim\!10^5$ to $\sim\!10^{11}$ He atoms, as obtained via titrations of the droplet beam with helium gas at room temperature. The measured peak flux is a factor of one thousand larger than in a continuous beam. Comparison with continuous nozzle results show similar droplet sizes at low T < 6 K, indicating in both cases the droplets are created via the fragmentation of the fluid.

Deleted: 12
Deleted: 05

Deleted: 2017

I. Introduction

Over the past two decades, helium (He) droplets have been widely used for laser spectroscopic studies of molecules, molecular and atomic clusters.[1-5] Molecular species isolated in cold (~0.4 K) and weakly interacting droplets often demonstrate well resolved vibrational spectra from which the structural information could be inferred. On the other hand, resolved rotational spectra have been used to study interaction of molecules with the superfluid environment.[1,5-7] Experiments with simple molecules and small (N < 10) clusters [8-10] employ smaller He droplets that are a few nanometer in diameter and contain up to about 10⁴ atoms. More recently, helium droplets were used to form large atomic and molecular clusters containing thousands to millions of particles, which were studied via spectroscopy in situ as well as by electron microscopy upon surface deposition. [11-14] Due to low evaporation enthalpy of liquid helium of ~7 K per atom, to sustain evaporative losses, the number of helium atoms in the droplets must be a factor of ~1000 larger that the number of the embedded particles. Capture of protein ions also requires a sufficiently large droplet.[15] Recent diffraction experiments with 100 nm sized doped droplets with an X-ray free electron laser (XFEL) demonstrated the emergence of quantized vortices in superfluid helium droplets [16] and enabled study of atomic aggregation mediated by quantum vortices.[17-19] Such studies demand the production of a large droplet with average number of atoms, $\langle N_{He} \rangle > 10^7$.

Helium droplets are produced from cryogenic expansion of pressurized helium in vacuum; larger droplets are formed at lower nozzle temperature. Most of the experiments up to date involve continuous nozzle beam expansion technique, which is well-characterized [20-23] and covers droplet sizes from ~ 100 to $\sim 10^{12}$ atoms. Pulsed droplet sources [24-27] are advantageous for studies involving pulsed techniques, such as laser-induced fluorescence, photo ionization or X-ray coherent diffraction imaging. Pulsed nozzles, which usually contain an electromagnetic valve, however, are difficult to run at the low temperatures of T < 6 K required for production of large droplets due to heat evolved during their operation. Nevertheless, experiments with helium droplets involving pulsed cryogenic nozzles are emerging. [15,20,26-32] Most of the groups employing pulsed valve use so called Even-Lavie valve[24,27,32-34],

Deleted: operate

which is rather expensive and difficult to acquire. Recent study with Even-Lavie valve reports sizes of $\sim 10^{10}$ atoms at the lowest temperature of 5 K.[32]

We have continued the development of the alternative pulsed valve technique which is based on a commercially available Parker Series 99 electromagnetic valve with 0.5 or 1 mm diameter.[15,20,26,29,31] Here, we report on the formation of pulses of large sized helium droplets, $\langle N_{He} \rangle = 10^5 - 10^{11}$, which were obtained at stagnation pressures of 5 and 10 bar and temperatures of 4 - 15 K. The low operation temperature is achieved upon confining the valve within a copper shroud in thermal contact with second stage of the closed cycle refrigerator. The average droplet sizes are obtained by attenuation of the droplet beam with collisional helium gas at room temperature as described by Gomez *et al.*[20] Additionally, the pulsed helium droplet beam intensity is measured and compared with the previous results with a continuous source.

II. Experiment

A schematic of the molecular beam setup is shown in Figure 1. It comprises of a source chamber which hosts a close cycle refrigerator (Sumitomo, RDK-408D). The droplets are produced by expanding high purity (99.9999%) helium at stagnation pressure P₀ and temperature T₀ into vacuum. We employed a Series 99 Parker (formerly General Valve) valve equipped with coppers gaskets and a Kel-F poppet which is operated by IOTA-ONE (General Valve) external driver. The valve consists of a body and a faceplate. The body accommodates a solenoid which holds an iron cylinder with attached spring and a poppet. The tip of the poppet sits on the orifice of the faceplate. The 1 mm (0.5 mm) orifice has a conical opening with angle of ~90°. Upon application of the electric pulse to solenoid, the poppet moves back, letting helium flow through the orifice, see Ref. [26] for more details. The central part of the beam is isolated by a 2 mm diameter skimmer placed at ~ 15 cm downstream from the nozzle. After passing through the skimmer, the beam enters the 0.82 m long pickup chamber. Further downstream, the beam passes through a gate valve and enters a UHV detection chamber containing an axial quadrupole mass spectrometer (QMS) (Extranuclear laboratories, 020-1) equipped with an electron impact ionizer. The QMS ionizer resides 130 cm downstream from the nozzle. The default ionization current and energy were set to 5 mA and 100 eV, respectively. The QMS is employed to measure intensities and the time of flight profiles of the droplet beam. The pressures in the vacuum

Deleted: 12

Deleted: 05

chambers were monitored by hot cathode ion gauges. The pickup chamber is additionally equipped with a fast ion gauge, which is used for the droplet flux measurements as described in the following Section.

The average droplet sizes were determined via attenuation of helium droplet beam by collisional He gas, as developed previously in Ref.[20] for continuous beams. During the attenuation experiments, the pickup chamber is flooded with He gas, which enters through a leak valve. The droplets encounter multiple collisions with the helium atoms as they pass through the pickup chamber leading to decrease of the average droplet size and concomitant decrease of the droplet beam intensity, as dictated by the collisional cross-section. The change of the He droplet beam intensity upon increasing of the pressure of the He collision gas in the pickup chamber is monitored by QMS which was tuned to detect mass m = 8 due to He₂⁺ splitter ions.

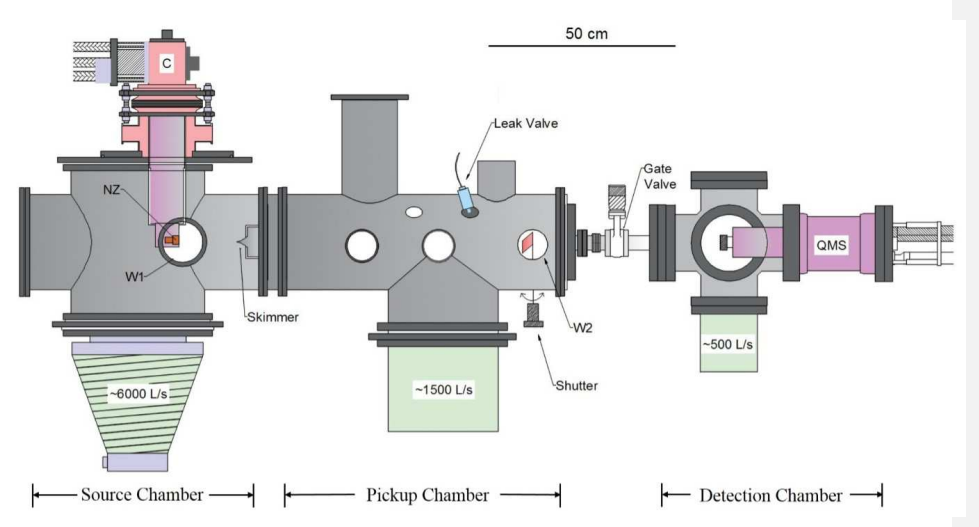


Figure 1. Schematic of the He droplet setup. The source chamber on the left hosts pulsed valve nozzle (NZ) attached to a cold head (C). It is backed by a 3000 L/s diffusion pump. The droplets pass through a 2 mm skimmer into the pickup chamber where the collisional He gas is introduced through a leak valve. This chamber is backed by a 1500 L/s turbomolecular pump. The pickup chamber also hosts a fast ion gauge (not shown) and a shutter for beam block. The droplets enter the UHV detection chamber through a 5 mm orifice and a gate valve where the helium ions are produced and detected by an axial quadrupole mass spectrometer (QMS). W1 and W2 are optical windows.

Deleted: 12

Deleted: 05

A three dimensional rendering of the adapter of valve to the cold head is presented in Figure 2. The adapter has a copper cylinder body with a flat rectangular face (Figure 2 (c)). The top of this design attaches to the second stage of the cold head, as shown in Figure 2 (f). The bottom end is covered by a copper lid (Figure 2 (d)). The rectangular face has two circular cavities. The outer cavity ensures proper fitting of the valve face plate while the inner cavity extends further inside the body of the cylinder. This extension provides contact between the valve body and the surrounding copper for efficient heat exchange. Once the valve is secured in place with screws, an auxiliary copper slab (outer cover in Figure 2 (f)) with a conical opening is placed in front of the faceplate and secured with bolts for better heat exchange between the valve face plate and the cold source. The He inlet line runs from the top of the cold head down to the bottom where the copper part is attached. It is coiled around the copper assembly from outside through 3 turns before it enters through a hole and attaches to the valve (Figure 2 (d)). Temperature is monitored by two silicon diode sensors: the first is placed on the second stage of the cryostat (Figure 2b), whereas the second is attached to the supply line of the pulsed valve (Figure 2(d)). The nozzle temperatures, T₀, reported in this paper are measured from the second silicon diode which gives the true reading of the gas temperature. The temperature is controlled through resistive heating. The temperature measured with the second sensor is higher than with the first one, due to the finite heat conductivity between the adapter assembly and the cold head.

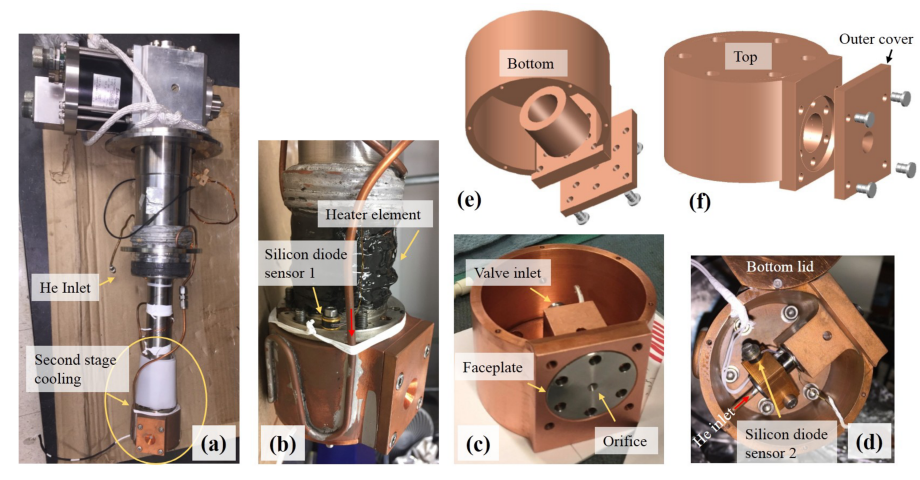


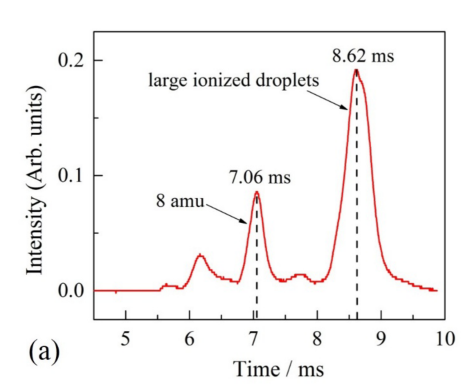
Figure 2. A schematic of the pulsed valve adapter. (a) The entire assembly attached to the cold head. (b) Zoomed image of the bottom part in (a). (f) The top view of the copper assembly along with the front cover. (c), (d), (e) The bottom view of the copper assembly. The nozzle valve fits in with the faceplate in the front. The valve inlet is attached to the helium line, as shown in (d) and a temperature sensor is placed on top of the connection. A thin copper lid closes the assembly (f).

Deleted: 12
Deleted: 05
Deleted: 2017

Deleted: A comparison between the two readings estimates the efficiency of thermal cooling



Deleted: 12
Deleted: 05
Deleted: 2017



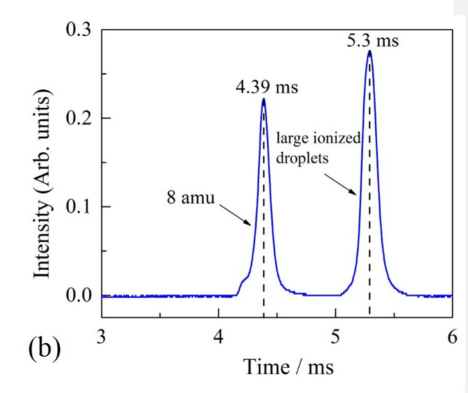


Figure 3. Time of flight spectrum as measured with QMS at nominal M=8 at two different repetition rates: 1 Hz and 20 Hz, at lowest operational $T_0=4.4$ K (1 Hz) and $T_0=5.7$ K (20 Hz) as indicated in panels (a) and (b), respectively. $P_0=5$ bar, Nominal pulse duration 160 μ s. The time zero corresponds to the falling edge of the nozzle driving pulse.

III. Results

Figure 3 (a) and (b) show the time dependence of the QMS signal at mass 8, I_8 , as measured at the two repetition rates of 1 Hz and 20 Hz, respectively, and lowest temperature with heater off. Figure 3 (b) shows two prominent peaks. The peak at the earlier arrival time of 4.39 ms corresponds to the He_2^+ ions ejected from the droplet after electron impact. The peak at the later time of 5.3 ms corresponds to larger mass (>>300 amu) of ionized droplets that are barely deflected by the mass filter and continue propagating along the quadrupole axis and are finally detected by an electron multiplier at the rare end of the QMS as has been observed previously.[35] Similar time dependence is observed at lowest temperature in Fig. 3 (a), which also shows two peaks at 7.06 ms and 8.62 ms. In addition, Figure 3 (a) has weaker peaks at shorter delay time of ~ 6.2 ms and ~ 7.7 ms are likely due to smaller faster droplets which may be created either at the beginning or at the end of the pulse. The width (FWHM) of the mass 8 peak at $T_0 = 4.4$ K is ~ 0.27 ms, about twice as broad as at $T_0 = 5.7$ K. The velocities of the droplets in (a) and (b) were estimated from the flight time of the faster peaks to be 184 m/s and 296 m/s, respectively. Figure 4 shows the temperature dependence of the droplet velocity as measured at $P_0 = 10$ bar.

Deleted: a

Deleted: which most likely arises from a broad size distribution from the output of the nozzle at 1 Hz





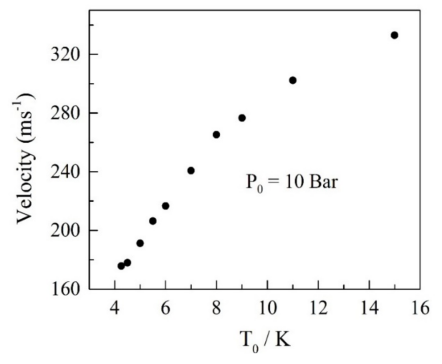


Figure 4. Helium droplet velocity as a function of temperature, T_0 . $P_0 = 10$ bar, $180 \mu s$, 1 Hz

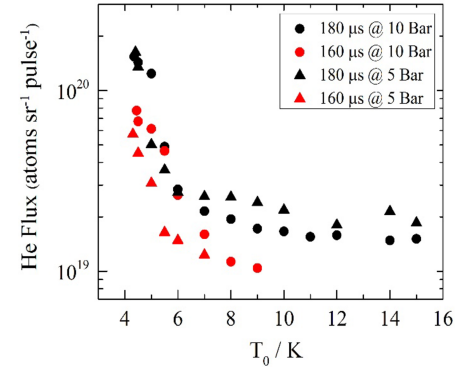


Figure 5. Helium flux measured at two different nozzle pulse duration of 160 μ s and 180 μ s and at P_0 =5 bar and 10 bar, as indicated in the legend.

Figure 5 shows flux of the He atoms per pulse obtained from a 1 mm diameter nozzle at different temperatures and at repetition rate of 1 Hz as measured with a fast ion gauge. The amount of He in the pulse was calculated as a product of the temporary pressure rise and the volume of the pickup chamber of $_60$ L. The solid angle of the beam is defined by the skimmer to be $\sim 1.4 \times 10^{-4}$ sr . The measurements were done at two different nominal pulse durations of 160 μ s and 180 μ s, and at $P_0 = 5$ bar and 10 bar. For the same P_0 , the longer duration pulse produces higher flux, which reaches a maximum at $\sim 2 \times 10^{20}$ atoms sr⁻¹ pulse⁻¹ at 4.3 K. However, for the same duration of the pulse, a very similar flux was obtained at a different P_0 .

Deleted: s

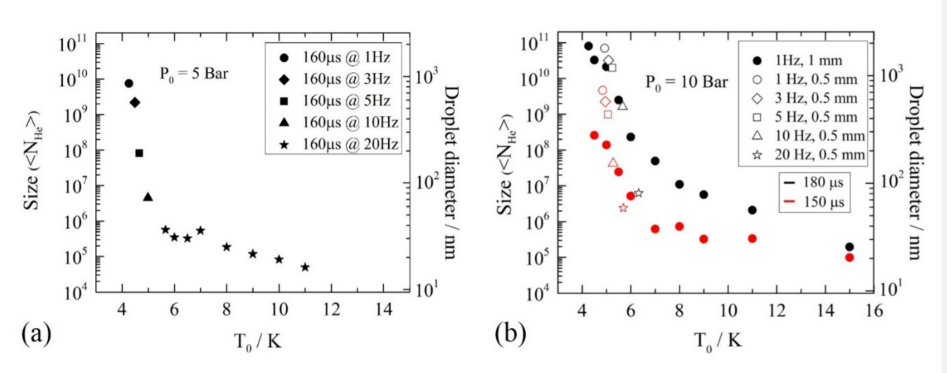


Figure 6. (a) Droplet sizes measured at different repetition rate for a pulse duration of $160~\mu s$ at $P_0=5$ bar with a 1 mm nozzle. Panel (b) shows sizes obtained at $P_0=10$ bar at 1 Hz with 1 mm nozzle for pulse durations, $180~\mu s$ and $150~\mu s$ as shown by filled black and red circles, respectively. Shown with open symbols are the sizes obtained with 0.5~mm diameter nozzle operating at the indicated repetition rate at lowest possible T_0 .

Figures 6 (a) and (b) show the results of measurements of the droplet sizes at $P_0 = 5$ bar and 10 bar, and for different indicated nominal nozzle pulse durations and at different repetition rates. The value of T₀ was varied from the lowest achievable temperature and upwards. It is seen that largest droplets containing about $10^{10} - 10^{11}$ atoms are obtained at $T_0 < 5.5$ K and at longer pulse duration of 180 μs. Figure 5 (b), shows that upon increase of T₀ the average droplet size decreases monotonously. In particular, at $T_0 > 6$ K, the size becomes less than $\sim 10^7$. The measurements at higher $P_0 = 10$ bar show a factor of about 10 larger droplet sizes at the same T_0 as compared to measurements at $P_0 = 5$ bar. In addition, measurements at 10 bar show a little kink at 6 bar, with weaker droplet size dependence at lower temperatures. Longer open pulse durations produce larger sized droplets, as evident in Figures 6 (a) and (b). The pulse duration is eventually limited by the pressure rise in the source chamber, leading to overwhelming of the pumping system. Figure 6 (a) shows the sizes obtained at different repetition rates from 1 Hz to 20 Hz at 5 bar and 160 µs. The lowest temperature in each case corresponds to the measurements with heater off. Higher repetition rate leads to a proportionally larger heat release and thus to higher minimal attainable T₀. As a result, when increasing the nozzle repetition rate, a steep decrease in the droplet size is observed. At 20 Hz, which is desirable for typical laboratory experiments involving lasers, the nozzle could be cooled down to 6 K. Open symbols in Figure 6 (b) show the average droplet sizes as measured with the 0.5 mm diameter nozzle at the lowest

Deleted: 12
Deleted: 05

attainable T_0 for the corresponding repetition rate. The results with 0.5 mm nozzle follow a similar progression as seen with the 1 mm diameter nozzle. Comparison within Figure 6 (b) shows that similar droplet sizes could be obtained with different diameter nozzles.

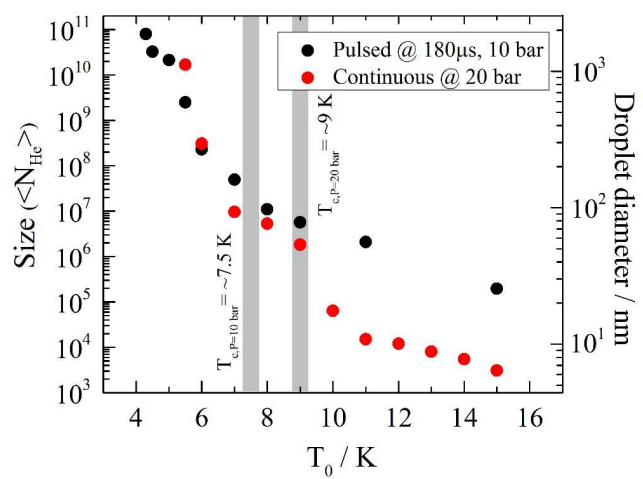


Figure 7. Droplet size from a continuous [20,36,37] and a pulsed sources. Vertical shaded lines show the temperatures of the critical isentropes at 10 and 20 bar.[38,39]

IV. Discussion

Figure 7 presents the comparison of the average droplet sizes obtained in this work with 1 mm nozzle at 10 bar and from 5 μ m continuous nozzle at 20 bar.[20] It is seen that at $T_0 > 9$ K, the pulsed nozzle produces larger droplets of about $10^6 - 10^7$. At lower $T_0 = 5$ -9 K however, droplets of comparable sizes could be obtained from the pulsed and continuous sources. Pulsed measurements at $P_0 = 20$ bar could not be carried out at high repetition rates due to overwhelming of the pumping system. At 10 bar, the continuous nozzle results are expected to be shifted by about 1-2 K towards lower temperatures. The largest droplets were obtained at the lowest $T_0 \sim 4$ K, are comparable in size to previous observations in other groups.[15,32]

The behavior of the continuous nozzle expansion in Figure 7 has been discussed in Refs.[20,22] With decreasing of T_0 from 15 to $\sim \! 10$ K, the average droplet size increases

Deleted: 12 Deleted: 05

gradually from ~10³ to 5×10⁴. The sharp jump in droplet size upon cooling from 10 K and 9 K signifies change of the expansion mode from subcritical to supercritical, where the expansion isentropes cut the liquid-vapor separation line from the gas- and liquid-side, respectively.[20,22] In supercritical expansion, the droplets are formed upon fragmentation of a fluid, giving rise to larger sizes. At 10 bar, the critical isentrope corresponds to a temperature of ~ 7.5 K.[38,39] However, the pulsed results in Figure 7 show no indication of any peculiarity in this region. The absence of the singularity in the region of the critical isentrope in the pulsed expansion is puzzling. The sharp rise of the droplet size upon temperature drop below the critical isentrope temperature is well documented at different expansion pressures in case of the continuous nozzle expansion.[1,22] The most obvious difference between the continuous and pulsed expansion is in the time helium stays in the high pressure expansion region, which scales with the nozzle diameter. Due to much larger diameter of the pulsed nozzle of 0.5 or 1 mm as compared with 5 μm for the continuous one, the time helium spends in the high pressure expansion region is ~100 times longer in the case of pulsed expansion. Longer "ripening" time may lead to longer growth and formation of larger droplets than in the continuous expansion. On the other hand, droplets of similar size are produced in the supercritical expansion regime at $T_0 < 9$ K in both the continuous and pulsed expansion. This likely indicates that, at low temperatures, the droplet formation in both cases includes the breakup of the fluid when the expansion crosses liquid-vapor separation line, whereas the secondary processes such as droplet growth or evaporation due to collisions with the He gas in the expansion region are of minor importance. The detailed kinetics of the

The large increase of the droplet flux at $T_0 < 6$ K (see Figure 4) is consistent with the formation of the collimated jet of very large droplets. At temperatures lower than critical (5.2 K), the valve is filled with liquid helium. A pulse extrudes some amount of liquid in vacuum, which could be estimated to be about 0.7 bar×cm³/pulse (at $P_0 = 10$ bar, $T_0 = 4.3$ K, 1 mm nozzle, 180 μ s pulse) as measured from the discharge rate of the fore vacuum pump. For comparison, the discharge rate through the continuous nozzle at $T_0 < 5$ K is ~3 bar×cm³/s. The discharge per pulse corresponds to a liquid volume of 1.1×10^{-3} cm³ at 4.5 K,[38] which is much smaller than the volume of the valve of ~ 1 cm³. At a higher repetition rate and at $T_0 < 5$ K, we have observed instabilities in the time of arrival of the pulses (Figure 3 (a)). This instability likely signifies that helium inside the valve separates into liquid and gas phases which may fluctuate from pulse to

droplet formation in the pulsed expansion remains to be studied.

Deleted: 12
Deleted: 05

Deleted: 2017

Deleted: about 2

pulse. Thus, when operating the valve at $T_0 < 5$ K, one should assure that helium remains liquid, which may require repetition rate limitation.

The results in Figure 5 enable estimating the pulse flux of the helium atoms at $T_0 < 5$ K to be $\sim 10^{24}$ atoms×sr⁻¹×s⁻¹ which is three orders of magnitude larger than $\sim \sim 10^{21}$ atoms×sr⁻¹×s⁻¹ in continuous beam [20]. This result has been validated in earlier experiments as well.[26,27,31] The increase is however still a factor of ~ 50 smaller than an estimate based on the ratio of the pulsed and continuous nozzle diameters, indicating that the beam from the pulsed nozzle is likely less collimated.

V. Conclusions

Here, we studied the production of large helium droplets in the pulsed cryogenic nozzle beam expansion. The average droplet sizes were obtained from attenuation of the droplet beam by collisional helium gas at room temperature. Careful design of the heat adapter allowed the nozzle to operate down to T₀ ≈ 4 K, enabling production of micron sized droplets, comparable to earlier measurements from a continuous nozzle. We found that the pulsed source covers the range of droplet sizes of 10⁵-10¹¹ for temperatures from 15 K to 4 K, which is comparable to that in the continuous beams at somewhat lower temperatures. On the other hand, the pulsed beam has a factor of ~ 1000 higher peak flux than previously found in continuous beams. Comparison with continuous nozzle results show similar droplet sizes at low T₀ < 6 K, indicating in both cases the droplets are created via the fragmentation of the fluid. However, a factor of ~ 100 larger droplets are produced in pulsed expansion at higher temperatures, which is assigned to correspondingly longer ripening time as compared with the continuous expansion. At the lowest T₀ required for producing very large droplets (>10⁷), the repetition rate is limited to about 5 Hz, which leaves scope for future valve improvements. Pulsed beams of large helium droplets may find wide applications in diverse spectroscopic and diffraction experiments with large molecules or clusters.

Deleted: 12

Deleted: 05

Deleted: 12
Deleted: 05
Deleted: 2017

VI. Acknowledgements

This research was supported through National Science Foundation Grant CHE-1664990. The authors are thankful to Sean O'Connell and Rico Mayro Tanyag for careful reading of the manuscript.

VII. References

- [1] J.P. Toennies, A.F. Vilesov, "Superfluid helium droplets: A uniquely cold nanomatrix for molecules and molecular complexes", Angew. Chem. Int. Ed. 43 (2004) 2622.
- F. Stienkemeier, K.K. Lehmann, "Spectroscopy and dynamics in helium nanodroplets", J. Phys. B: At. Mol. Opt. Phys. 39 (2006) R127.
- [3] J. Tiggesbaumker, F. Stienkemeier, "Formation and properties of metal clusters isolated in helium droplets", Phys. Chem. Chem. Phys. 9 (2007) 4748.
- [4] C. Callegari, W.E. Ernst, Handbook of High Resolution Spectroscopy, John Wiley & Sons, Chichester, 2011 1551.
- [5] M.Y. Choi, G.E. Douberly, T.M. Falconer, W.K. Lewis, C.M. Lindsay, J.M. Merritt, P.L. Stiles, R.E. Miller, "Infrared spectroscopy of helium nanodroplets: novel methods for physics and chemistry", Int. Rev. Phys. Chem. 25 (2006) 15.
- [6] S. Grebenev, M. Hartmann, M. Havenith, B. Sartakov, J.P. Toennies, A.F. Vilesov, "The rotational spectrum of single OCS molecules in liquid ⁴He droplets", J. Chem. Phys. 112 (2000) 4485
- [7] M. Hartmann, R.E. Miller, J.P. Toennies, A. Vilesov, "Rotationally resolved spectroscopy of SF₆ in liquid-helium clusters A molecular probe of cluster temperature", Phys. Rev. Lett. 75 (1995) 1566
- [8] S.D. Flynn, D. Skvortsov, A.M. Morrison, T. Liang, M.Y. Choi, G.E. Douberly, A.F. Vilesov, "Infrared spectra of HCl-H₂O clusters in helium nanodroplets", J. Phys. Chem. Lett. 1 (2010) 2233.
- [9] H. Hoshina, M. Slipchenko, K. Prozument, D. Verma, M.W. Schmidt, J. Ivanic, A.F. Vilesov, "Infrared spectroscopy and structure of (NO)_n clusters", J. Phys. Chem. A 120 (2016) 527.
- [10] T. Liang, P.L. Raston, G.E. Douberly, "Helium nanodroplet isolation spectroscopy and ab initio calculations of HO₃-(O₂)_n clusters", ChemPhysChem 14 (2013) 764.
- [11] E. Loginov, L.F. Gomez, A.F. Vilesov, "Surface deposition and imaging of large Ag clusters formed in He droplets", J. Phys. Chem. A 115 (2011) 7199.
- [12] V. Mozhayskiy, M.N. Slipchenko, V.K. Adamchuk, A.F. Vilesov, "Use of helium nanodroplets for assembly, transport, and surface deposition of large molecular and atomic clusters", J. Chem. Phys. 127 (2007) 094701.
- [13] E. Latimer, D. Spence, C. Feng, A. Boatwright, A.M. Ellis, S.F. Yang, "Preparation of ultrathin nanowires using superfluid helium droplets", Nano. Lett. 14 (2014) 2902.
- [14] A. Volk, P. Thaler, M. Koch, E. Fisslthaler, W. Grogger, W.E. Ernst, "High resolution electron microscopy of Ag-clusters in crystalline and non-crystalline morphologies grown inside superfluid helium nanodroplets", J. Chem. Phys. 138 (2013) 214312.
- [15] F. Bierau, P. Kupser, G. Meijer, G. von Helden, "Catching proteins in liquid helium droplets", Phys. Rev. Lett. 105 (2010) 133402.

- L.F. Gomez, K.R. Ferguson, J.P. Cryan, C. Bacellar, R.M.P. Tanyag, C. Jones, S. Schorb, D. Anielski, A. Belkacem, C. Bernando, R. Boll, J. Bozek, S. Carron, G. Chen, T. Delmas, L. Englert, S.W. Epp, B. Erk, L. Foucar, R. Hartmann, A. Hexemer, M. Huth, J. Kwok, S.R. Leone, J.H.S. Ma, F.R.N.C. Maia, E. Malmerberg, S. Marchesini, D.M. Neumark, B. Poon, J. Prell, D. Rolles, B. Rudek, A. Rudenko, M. Seifrid, K.R. Siefermann, F.P. Sturm, M. Swiggers, J. Ullrich, F. Weise, P. Zwart, C. Bostedt, O. Gessner, A.F. Vilesov, "Shapes and vorticities of superfluid helium nanodroplets", Science 345 (2014) 906.
- [17] C. Bernando, R.M.P. Tanyag, C. Jones, C. Bacellar, M. Bucher, K.R. Ferguson, D. Rupp, M.P. Ziemkiewicz, L.F. Gomez, A.S. Chatterley, T. Gorkhover, M. Muller, J. Bozek, S. Carron, J. Kwok, S.L. Butler, T. Moller, C. Bostedt, O. Gessner, A.F. Vilesov, "Shapes of rotating superfluid helium nanodroplets", Phys. Rev. B 95 (2017) 064510.
- [18] C.F. Jones, C. Bernando, R.M.P. Tanyag, C. Bacellar, K.R. Ferguson, L.F. Gomez, D. Anielski, A. Belkacem, R. Boll, J. Bozek, S. Carron, J. Cryan, L. Englert, S.W. Epp, B. Erk, L. Foucar, R. Hartmann, D.M. Neumark, D. Rolles, A. Rudenko, K.R. Siefermann, F. Weise, B. Rudek, F.P. Sturm, J. Ullrich, C. Bostedt, O. Gessner, A.F. Vilesov, "Coupled motion of Xe clusters and quantum vortices in He nanodroplets", Phys. Rev. B 93 (2016) 180510(R).
- [19] R.M.P. Tanyag, C. Bernando, C.F. Jones, C. Bacellar, K.R. Ferguson, D. Anielski, R. Boll, S. Carron, J.P. Cryan, L. Englert, S.W. Epp, B. Erk, L. Foucar, L.F. Gomez, R. Hartmann, D.M. Neumark, D. Rolles, B. Rudek, A. Rudenko, K.R. Siefermann, J. Ullrich, F. Weise, C. Bostedt, O. Gessner, A.F. Vilesov, "Communication: X-ray coherent diffractive imaging by immersion in nanodroplets", Struct. Dyn. 2 (2015) 051102.
- [20] L.F. Gomez, E. Loginov, R. Sliter, A.F. Vilesov, "Sizes of large He droplets", J. Chem. Phys. 135 (2011) 154201.
- [21] U. Henne, J.P. Toennies, "Electron capture by large helium droplets", J. Chem. Phys. 108 (1998) 9327.
- [22] H. Buchenau, E.L. Knuth, J. Northby, J.P. Toennies, C. Winkler, "Mass-spectra and time-of-flight distributions of helium cluster beams", J. Chem. Phys. 92 (1990) 6875.
- [23] R. Sliter, L.F. Gomez, J. Kwok, A. Vilesov, "Sizes distributions of large He droplets", Chem. Phys. Lett. 600 (2014) 29.
- [24] R. Katzy, M. Singer, S. Izadnia, A.C. LaForge, F. Stienkemeier, "Doping He droplets by laser ablation with a pulsed supersonic jet source", Rev. Sci. Instrum. 87 (2016) 013105.
- [25] F. Stienkemeier, A.F. Vilesov, "Electronic spectroscopy in He droplets", J. Chem. Phys. 115 (2001) 10119.
- [26] M.N. Slipchenko, S. Kuma, T. Momose, A.F. Vilesov, "Intense pulsed helium droplet beams", Rev. Sci. Instrum. 73 (2002) 3600.
- [27] D. Pentlehner, R. Riechers, B. Dick, A. Slenczka, U. Even, N. Lavie, R. Brown, K. Luria, "Rapidly pulsed helium droplet source", Rev. Sci. Instrum. 80 (2009) 043302.
- [28] A.I.G. Florez, D.S. Ahn, S. Gewinner, W. Schollkopf, G. von Helden, "IR spectroscopy of protonated leu-enkephalin and its 18-crown-6 complex embedded in helium droplets", Phys. Chem. Chem. Phys. 17 (2015) 21902.
- [29] V. Ghazarian, J. Eloranta, V.A. Apkarian, "Universal molecule injector in liquid helium: Pulsed cryogenic doped helium droplet source", Rev. Sci. Instrum. 73 (2002) 3606.
- [30] Y.T. He, J. Zhang, Y. Li, W.M. Freund, W. Kong, "Facile time-of-flight methods for characterizing pulsed superfluid helium droplet beams", Rev. Sci. Instrum. 86 (2015) 084102.
- [31] S.F. Yang, S.M. Brereton, A.M. Ellis, "Controlled growth of helium nanodroplets from a pulsed source", Rev. Sci. Instrum. 76 (2005) 104102.
- [32] D. Rupp, N. Monserud, B. Langbehn, M. Sauppe, J. Zimmermann, Y. Ovcharenko, T. Moller, F. Frassetto, L. Poletto, A. Trabattoni, F. Calegari, M. Nisoli, K. Sander, C. Peltz, M.J. Vrakking, T. Fennel, A. Rouzee, "Coherent diffractive imaging of single helium nanodroplets with a high harmonic generation source", Nat. Commun. 8 (2017) 493.

Deleted: 12
Deleted: 05
Deleted: 2017

- [33] U. Even, ""The Even-Lavie valve as a source for high intensity supersonic beam", EPJ Tech. Instrum. 2 (2015) 17.
- [34] V. Kumarappan, C.Z. Bisgaard, S.S. Viftrup, L. Holmegaard, H. Stapelfeldt, "*Role of rotational temperature in adiabatic molecular alignment*", J. Chem. Phys. 125 (2006) 194308.
- [35] J. Fine, D. Verma, C. Jones, C. Wittig, A.F. Vilesov, "Formation of He₄⁺ via electron impact of helium droplets", J. Chem. Phys. (2017) submitted.
- [36] M. Lewerenz, B. Schilling, J.P. Toennies, "A new scattering deflection method for determining and selecting the sizes of large liquid clusters of ⁴He", Chem. Phys. Lett. 206 (1993) 381.
- [37] B. Schilling, Ph.D dissertation (University of Göttingen), Max-Planck-Institut für Strömungsforschung, Göttingen, Germany, 1993.
- [38] R.D. McCarty, "Thermodynamic Properties of Helium 4 from 2 to 1500 K at Pressures to 10⁸ Pa", J. Phys. Chem. Ref. Data 2 (1973) 923.
- [39] J. Harms, J.P. Toennies, E.L. Knuth, "Droplets formed in helium free-jet expansions from states near the critical point", J. Chem. Phys. 106 (1997) 3348.

Deleted: 12
Deleted: 05
Deleted: 2017